MINERALOGICAL JOURNAL, VOL. 13, NO. 7, PP. 424–433, JULY 1987

Hollandite and cryptomelane in the manganese oxide deposits of the Sausar Group, India

Hiroyuki MIURA, Himadri BANERJEE*, Yu HARIYA, Somnath DASGUPTA and Supriya ROY****

*Department of Geology and Mineralogy, Hokkaido University, Sapporo 060, Japan and **Department of Geological Sciences, Jadavpur University, Calcutta 700032, India*

Abstract

The phase chemistry and the structure of hollandite-cryptomelane series in the Precambrian Sausar Group of India are reinvestigated. The tunnel-cations of the hollandite-cryptomelane series of the present investigation do not show complete exchanges. Crystal symmetry of these minerals is affected by the amounts and the composition of the tunnel cations. With increasing Ba^{2+} content, symmetry of cryptomelane in Tirodi area changes from tetragonal to monoclinic. These minerals appear to have been formed in a wide range of metamorphic grade from the lowest (chlorite-biotite) to the highest (sillimanite) grades. The local breakdown of hollandite to hausmannite ±Ba-feldspar must have occurred by the change of f_{O_2} condition of the system during metamorphism.

Introduction

In the Precambrian Sausar Group of India (846-986 Ma.), the manganese oxide orebodies are commonly interbanded with manganese oxide-silicate rocks (gondite) and manganese silicate-carbonate-oxide rocks. These usually occur enclosed within the non-carbonatic and dominantly metapelite-bearing Mansar Formation (Roy, 1966 and 1981). The metapelites, manganese oxides and the gondites had identical thermal and deformational histories and they have been metamorphosed under different physico-chemical conditions, from greenschist to amphibolite facies (Roy, 1966 and 1981; Dasgupta *et al.*, 1984). The f_{O_2} was buffered internally and varied considerably within the adjacent bands of manganese oxides, manganese oxide-silicate, manganese silicate-carbonate-oxide rocks and the metapelites (Dasgupta and Manickavasagam, 1981; Dasgupta *et al.*, 1984 and 1985). Bhattacharya *et al.* (1984) have classified the manganese oxide ores into two types as hollandite-bearing and hollandite-free assemblages. In both cases a progressive deoxidation with rise of temperature has been noted. They have also observed the breakdown of hollandite into hausmannite +

*Present address: Department of Geological Sciences, Jadavpur University, Calcutta 700032, India

Ba-feldspar at the peak of metamorphism.

Hollandite was first reported from this belt by Fermor in 1906 (Roy, 1981). Roy (1966 and 1981) found that hollandite from Sausar belt is very rich in Ba^{2+} ion with insignificant amount of K^+ ion. Bhattacharya *et al.* (1984), however, reported that hollandites of this belt are very high in K^+ ion content with fairly low Ba^{2+} ion. Cryptomelane has also been observed as a secondary phase in this belt (Roy, 1966 and 1981).

Byström and Byström (1950) first established the structure of the hollandite group minerals, as an isostructural series $A_{1-2}Mn_8O_{16}.nH_2O$. Their work has been supported by Burns and Burns (1977), Turner and Buseck (1979, 1981), Giovanoli (1980), Post *et al.* (1982), Burns *et al.* (1983, 1985) and Miura (1986). Keeping in view these earlier studies, we have reinvestigated the structure, chemistry and stability of the hollandite group of minerals from the Sausar belt. Also the nature of the gradation of exchangeable cations between the Ba^{2+} and K^+ end-member analogues has been probed.

Petrography and Phase Chemistry

The relevant petrographic features of the manganese ore bodies are as follows: i) the major associated phases in hollandite-bearing assemblages are; braunite$_1$*, ±bixbyite, braunite$_2$, ±hausmannite, hematite, quartz, and ±K-feldspar, ii) an early braunite$_1$ along with pyrolusite or hollandite was formed from appropriate precursors, during the early stage of metamorphism, iii) bixbyite developed in a relatively later stage with the complete disappearance of pyrolusite. Bixbyite was partly converted later to braunite$_2$ (bixbyite + quartz → braunite$_2$ ±hematite), iv) hausmannite has been observed only in the highest grade of metamorphism and was formed as a deoxidation product of bixbyite or hollandite, with the appearance of a Ba-bearing phase in the later case, v) in the hollandite-free assemblages, hausmannite occurs as crystallographically oriented lamellae within jacobsite (vredenbergite). These are the deoxidation products after bixbyite. The details of the phase assemblages from various metamorphic grades of the Sausar belt, along with the locality index are given in Table 1.

There are two types of band or lamination. One is rich in hollandite of high Ba^{2+}/K^+ ratio and the other is rich in cryptomelane of very low Ba^{2+}/K^+ ratio. Figures 1a and b show the colour macromaps of Ba^{2+} and K^+ contents in the specimen TI-5. It is clear from these figures that hollandite and cryptomelane occur in different parts as lamellae of the specimen. Metamorphic equilibration of these crypto-

*Braunite$_1$ is the early formed phase and braunite$_2$ developed at a later stage as the breakdown product of bixbyite.

TABLE 1. The phase assemblages in the manganese oxide deposits from Sausar group.

Smaple No.	B1	U4	CH1	CH2	CH2'	CH15	C11	C113	TI1	TI2	TI3	TI4	TI5	TI6	T3
Hollandite	-	+	-	-	-	+	-	+	+	-	-	+	+	-	+
Cryptomelane	+	-	+	+	+	-	+	-	+	+	+	-	+	+	-
Braunite	+	+	+	-	+	+	+	+	+	+	+	+	+	+	+
Bixbyite	±	+	-	+	+	+	+	+	±	+	+	-	+	+	+
K-feldspar	±		-	+	+	-			-	+	-	-	+	+	

Index: B1, U4-Balaghat and Ukwa area (chlorite-biotite grade);
CH1, CH2, CH2', CH15, C11, C113-Chikla area (staurolite-kyanite grade);
TI1, TI2, TI3, TI4, TI5, TI6, T3-Tirodi area (sillimanite grade).
Quartz and hematite (as minor globules, mainly) are ubiquitous phases in almost all the assemblages.
In TI1 and TI5, though hollandite and cryptomelane occur in the same sample, they are restricted to distinct laminations, free of one another, associated phases being similar. U4, C11, C113, T3-analyses are from Bhattacharya *et al.* (1984).

melane or hollandite and the associated braunite, bixbyite and other silicates is a common feature. This metamorphically recrystallized cryptomelane is different from the secondary cryptomelane observed from the oxidation zones of this belt (Roy, 1966 and 1981). The latter which usually occurs along fractures and cleavages of the Mn-oxides, at places pseudomorphing the grain boundary, generally has a crypto-crystalline nature and a very high H_2O content (Table 5). They will be referred as

TABLE 2. Chemical composition of hollandite.

Serial No.	1	2	3	4	5	6	7	8	9	10	11	12
Sample No.	U4	CH15	C113	T3	TI4	TI4	TI5	TI5	TI1	TI1	TI1	TI1
SiO_2	0.07	0.12	0.08	0.08	0.00	0.00	0.00	0.00	0.00	0.00	0.00	0.00
TiO_2	0.28	0.30	0.49	0.46	0.26	0.28	1.14	0.31	0.29	0.27	0.24	0.27
Al_2O_3	0.59	1.04	0.61	0.78	0.32	0.26	0.10	0.41	0.26	0.35	0.17	0.40
Cr_2O_3	----	0.00	----	----	0.00	0.05	0.00	0.01	0.02	0.00	0.00	0.02
Fe_2O_3	4.47	7.06	7.57	7.52	5.17	6.05	8.32	6.51	3.31	3.71	3.57	3.36
MnO_2	78.29	72.51	69.84	75.43	78.67	77.33	75.24	76.95	79.74	79.96	79.40	79.10
MgO	0.00	0.00	0.00	0.00	0.00	0.00	0.00	0.00	0.08	0.00	0.00	0.00
NiO	----	0.00	----	----	0.00	0.00	0.00	0.00	0.00	0.06	0.00	0.00
CaO	0.07	0.08	0.08	0.09	0.02	0.01	0.04	0.04	0.00	0.01	0.00	0.02
Na_2O	0.42	0.13	0.16	0.34	0.72	0.38	0.46	0.64	0.48	0.42	0.63	0.45
K_2O	2.60	0.09	0.29	1.99	1.86	1.66	2.44	2.06	1.31	1.60	1.40	1.29
BaO	10.06	18.90	18.17	11.52	9.74	11.21	8.88	9.97	12.92	10.81	12.11	12.11
Total	96.85	100.23	97.29	98.21	96.76	97.23	96.62	96.90	98.41	97.19	97.52	97.02
Si	0.009	0.016	0.011	0.011	0.000	0.000	0.000	0.000	0.000	0.000	0.000	0.000
Ti	0.028	0.031	0.051	0.046	0.026	0.028	0.113	0.031	0.029	0.027	0.023	0.027
Al	0.092	0.166	0.100	0.122	0.049	0.040	0.015	0.064	0.041	0.054	0.026	0.062
Cr	----	0.000	----	----	0.000	0.005	0.000	0.001	0.002	0.000	0.000	0.002
Fe^{3+}	0.445	0.718	0.795	0.747	0.514	0.604	0.829	0.649	0.329	0.368	0.356	0.337
Mn^{4+}	7.158	6.772	6.739	6.881	7.175	7.098	6.888	7.045	7.266	7.280	7.276	7.272
Mg	0.000	0.000	0.000	0.000	0.000	0.000	0.000	0.000	0.015	0.000	0.000	0.000
Ni	----	0.000	----	----	0.000	0.000	0.000	0.000	0.000	0.007	0.000	0.000
Ca	0.010	0.011	0.012	0.013	0.003	0.001	0.006	0.005	0.000	0.002	0.000	0.003
Na	0.108	0.034	0.043	0.088	0.183	0.098	0.119	0.165	0.122	0.106	0.162	0.115
K	0.439	0.015	0.052	0.335	0.313	0.281	0.412	0.348	0.220	0.268	0.237	0.218
Ba	0.521	1.001	0.994	0.596	0.504	0.583	0.461	0.517	0.667	0.558	0.629	0.631
Total	8.810	8.764	8.797	8.839	8.767	8.738	8.843	8.825	8.691	8.670	8.709	8.667

Note: Number of ions calculated on O = 16. Total Mn as MnO_2 and Fe as Fe_2O_3. Repeated sample numbers give the average analyses of several grains in the same sample. See Table 1 for sample indices and mineral assemblages.

TABLE 3. Chemical composition of cryptomelane.

Serial No.	1	2	3	4	5	6	7	8	9	10	11	12	13
Sample No.	B1	B1	B1	CH1	CH1	CH1	CH2	CH2	CH2	CH2'	CH2'	CH2'	C11
SiO_2	0.00	0.00	0.00	0.00	0.00	0.00	0.00	0.00	0.00	0.00	0.00	0.00	0.05
TiO_2	0.02	0.04	0.00	0.09	0.09	0.14	0.11	0.12	0.13	0.16	0.17	0.14	0.12
Al_2O_3	0.40	0.49	0.64	0.47	0.41	0.38	0.26	0.30	0.30	0.33	0.34	0.37	0.30
Cr_2O_3	0.03	0.00	0.00	0.00	0.01	0.01	0.00	0.02	0.01	0.00	0.00	0.01	----
Fe_2O_3	3.82	3.78	3.08	5.82	5.53	5.54	6.93	6.58	7.02	5.70	6.44	6.46	5.71
MnO_2	87.27	86.47	87.43	82.23	82.27	82.62	80.23	81.45	80.78	82.73	81.18	81.43	80.30
MgO	0.00	0.00	0.00	0.02	0.00	0.04	0.10	0.00	0.00	0.03	0.00	0.00	0.00
NiO	0.00	0.00	0.00	0.01	0.03	0.00	0.02	0.04	0.00	0.00	0.00	0.02	----
CaO	0.02	0.07	0.15	0.05	0.09	0.12	0.06	0.02	0.03	0.04	0.08	0.03	0.13
Na_2O	1.26	1.47	1.73	1.08	0.88	0.99	0.52	0.85	0.56	1.05	0.87	0.95	1.18
K_2O	6.73	6.95	6.37	4.79	3.80	4.57	3.88	4.55	4.34	5.18	4.76	4.66	4.51
BaO	1.36	1.32	1.26	4.59	4.13	3.53	5.71	4.35	5.05	3.00	4.23	4.45	3.70
Total	100.91	100.59	100.66	99.15	97.24	97.94	97.82	98.28	98.22	98.22	98.07	98.52	96.00
Si	0.000	0.000	0.000	0.000	0.000	0.000	0.000	0.000	0.000	0.000	0.000	0.000	0.006
Ti	0.001	0.004	0.000	0.008	0.008	0.013	0.011	0.012	0.012	0.015	0.016	0.013	0.011
Al	0.058	0.071	0.092	0.070	0.062	0.056	0.039	0.045	0.045	0.049	0.051	0.055	0.046
Cr	0.003	0.000	0.000	0.000	0.001	0.001	0.000	0.002	0.001	0.000	0.000	0.001	----
Fe^{3+}	0.349	0.347	0.282	0.551	0.529	0.526	0.668	0.627	0.672	0.539	0.615	0.615	0.555
Mn^{4+}	7.323	7.290	7.332	7.150	7.229	7.206	7.109	7.135	7.110	7.192	7.127	7.124	7.167
Mg	0.000	0.000	0.000	0.004	0.000	0.008	0.020	0.000	0.000	0.006	0.000	0.000	0.000
Ni	0.000	0.000	0.000	0.001	0.003	0.000	0.002	0.005	0.000	0.000	0.000	0.002	----
Ca	0.002	0.009	0.019	0.006	0.013	0.016	0.008	0.003	0.004	0.006	0.011	0.003	0.018
Na	0.296	0.347	0.408	0.264	0.216	0.243	0.129	0.209	0.138	0.256	0.215	0.233	0.295
K	1.043	1.082	0.986	0.769	0.616	0.735	0.635	0.736	0.706	0.830	0.771	0.753	0.743
Ba	0.065	0.063	0.060	0.226	0.206	0.175	0.287	0.216	0.252	0.148	0.210	0.221	0.187
Total	9.140	9.213	9.179	9.049	8.883	8.979	8.908	8.990	8.940	9.041	9.016	9.020	9.028

Note: Number of ions calculated on O = 16. Total Mn as MnO_2 and Fe as Fe_2O_3. Repeated sample numbers give the average analyses of several grains in the same sample. See Table 1 for sample indices and mineral assemblages.

TABLE 3. Chemical composition of cryptomelane (continuing).

Serial No.	14	15	16	17	18	19	20	21	22	23	24	25	26
Sample No.	TI1	TI2	TI2	TI2	TI5	TI5	TI5	TI3	TI3	TI3	TI6	TI6	TI6
SiO_2	0.00	0.00	0.00	0.00	0.00	0.00	0.00	0.00	0.00	0.00	0.00	0.01	0.00
TiO_2	0.01	0.08	0.07	0.04	0.00	0.09	0.05	0.02	0.00	0.06	0.19	0.15	0.22
Al_2O_3	0.34	0.35	0.26	0.46	0.28	1.09	0.72	0.11	0.05	0.01	0.89	0.80	0.77
Cr_2O_3	0.00	0.05	0.01	0.00	0.03	0.07	0.00	0.03	0.00	0.00	0.00	0.00	0.03
Fe_2O_3	3.86	6.98	5.35	6.12	3.39	3.52	3.68	5.38	5.96	6.20	3.98	2.62	4.56
MnO_2	86.52	80.63	83.48	80.93	85.91	84.50	83.66	82.67	82.68	82.98	85.32	86.69	83.15
MgO	0.01	0.03	0.00	0.00	0.02	0.03	0.00	0.04	0.00	0.00	0.00	0.08	0.00
NiO	0.00	0.00	0.01	0.00	0.00	0.02	0.00	0.00	0.00	0.05	0.01	0.02	0.01
CaO	0.06	0.05	0.03	0.06	0.02	0.05	0.02	0.08	0.06	0.04	0.04	0.09	0.09
Na_2O	1.44	0.74	1.08	0.85	1.31	1.29	1.16	0.94	0.91	0.85	1.35	1.29	1.41
K_2O	6.84	4.19	5.35	4.63	5.63	5.37	4.74	5.54	5.53	5.60	5.46	5.81	4.51
BaO	1.47	5.43	3.67	4.81	3.21	3.46	4.13	3.04	2.66	3.18	2.54	1.91	4.45
Total	100.55	98.53	99.31	97.90	99.80	99.49	98.16	97.85	97.85	98.97	99.78	99.47	99.20
Si	0.000	0.000	0.000	0.000	0.000	0.000	0.000	0.000	0.000	0.000	0.000	0.001	0.000
Ti	0.001	0.008	0.007	0.004	0.000	0.008	0.005	0.001	0.000	0.006	0.018	0.014	0.021
Al	0.049	0.053	0.039	0.069	0.041	0.160	0.107	0.016	0.007	0.002	0.129	0.116	0.114
Cr	0.000	0.005	0.001	0.000	0.003	0.007	0.000	0.003	0.000	0.000	0.000	0.000	0.003
Fe^{3+}	0.355	0.669	0.504	0.588	0.315	0.329	0.349	0.512	0.567	0.586	0.368	0.242	0.429
Mn^{4+}	7.305	7.090	7.215	7.139	7.348	7.240	7.288	7.233	7.222	7.195	7.250	7.353	7.189
Mg	0.002	0.005	0.000	0.000	0.004	0.006	0.000	0.008	0.000	0.000	0.000	0.015	0.000
Ni	0.000	0.000	0.001	0.000	0.000	0.002	0.000	0.000	0.000	0.005	0.001	0.002	0.001
Ca	0.007	0.007	0.004	0.009	0.002	0.007	0.003	0.011	0.008	0.006	0.006	0.012	0.012
Na	0.340	0.183	0.261	0.209	0.315	0.311	0.283	0.230	0.222	0.207	0.321	0.306	0.341
K	1.065	0.680	0.853	0.753	0.889	0.849	0.762	0.895	0.891	0.896	0.857	0.909	0.719
Ba	0.070	0.271	0.180	0.240	0.155	0.168	0.204	0.151	0.132	0.156	0.122	0.092	0.218
Total	9.194	8.971	9.065	9.011	9.072	9.087	9.001	9.060	9.049	9.059	9.072	9.062	9.047

"supergene cryptomelane" in the subsequent discussions.

Chemical analysis of the phases was carried out using EPMA (JCMA-733 model) with an accelerating voltage of 15kV, specimen current of 1×10^{-8}A and 10 μm electron beam diameter. Natural Fe_2O_3 and synthetic phases of other elements were

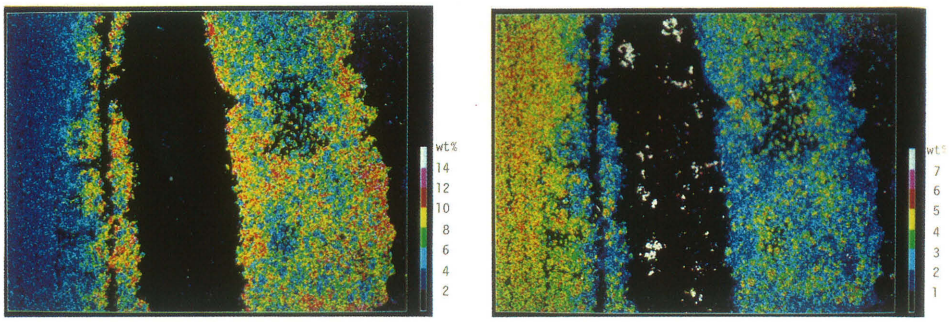

a b

FIG. 1. Colour macromaps of hollandite-cryptomelane lamellae from Tirodi mine (TI-5).
a) Ba wt %, b) K wt %.
size 1.35 x 1.20 cm (aspect ratio is not accurate because of the CRT display).

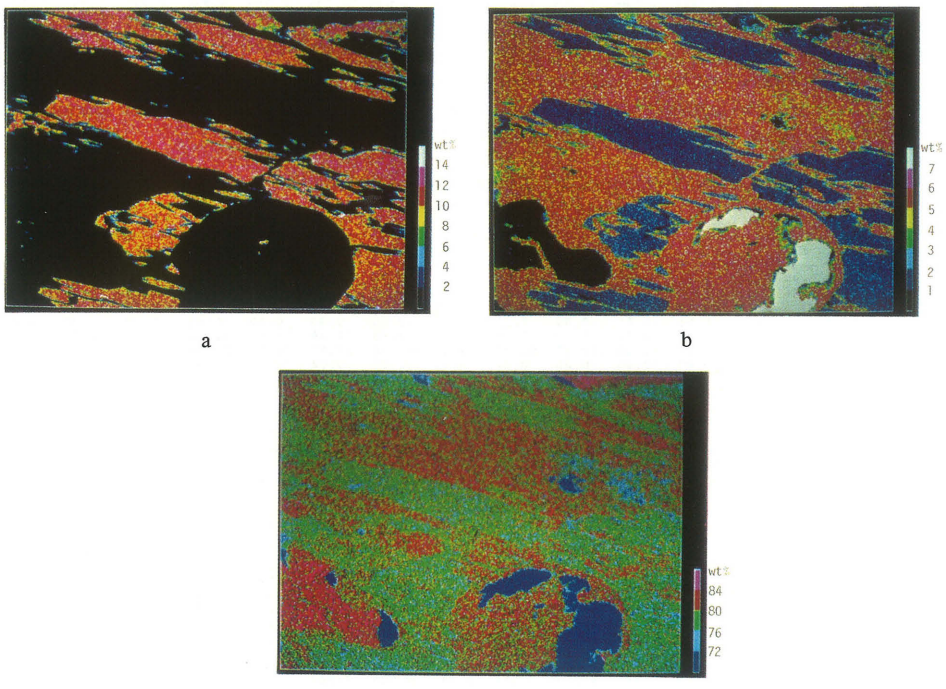

a b

c

FIG. 2. Colour macromaps of hollandite-cryptomelane series minerals being crystallized along the crack of braunite.
a) Ba wt %, b) K wt %, c) Mn wt %.
size 0.90 x 0.80 mm (aspect ratio is not accurate because of the CRT display).

used as standards. Oxide concentrating values were corrected using ZAF scheme. The compositions of hollandite and cryptomelane are presented in Tables 2 and 3 respectively. Between the coexisting grains of hollandite and cryptomelane and even within a single grain, the concentrations of A-cations vary considerably, indicating significant disordered nature of the tunnel cations. This fact indicates disequilibration in their chemical potential, even on a micro-environment. Hollandite and cryptomelane seem to be stable within a wide range from the lowest to the highest grades of metamorphism. These phases are anhydrous having only a very insignificant quantity of H_2O (Tables 2 and 3). Figure 3 shows that in a Ba^{2+}-K^+-Na^+ ternary field, the compositions of these phases can be plotted in two distinct regions of the hollandite and cryptomelane fields. Nambu and Tanida (1980) reported a complete gradation of chemical composition between cryptomelane and manjiroite. In the present study, the average number of A-cation of hollandite is nearly about 1, while it varies between 1.2 to 1.4 in case of cryptomelanes. The site occupancy limitations in the tunnel structure of these two phases, together with difference in the charge of the Ba^{2+} and K^+ ions and the overall charge balance between the tunnel cations and the $[MnO_6]$ octahedra, probably inhibited a complete gradation between the tunnel cations of these two phases (Byström and Byström, 1951; Burns and Burns, 1977; Giovanoli, 1980; Post *et al.*, 1982). Giovanoli (1980) and Giovanoli and Balmer (1981) studied on synthetic phases and reported that the replacement between Ba^{2+} and K^+ ions in this isostructural group is only of limited extent.

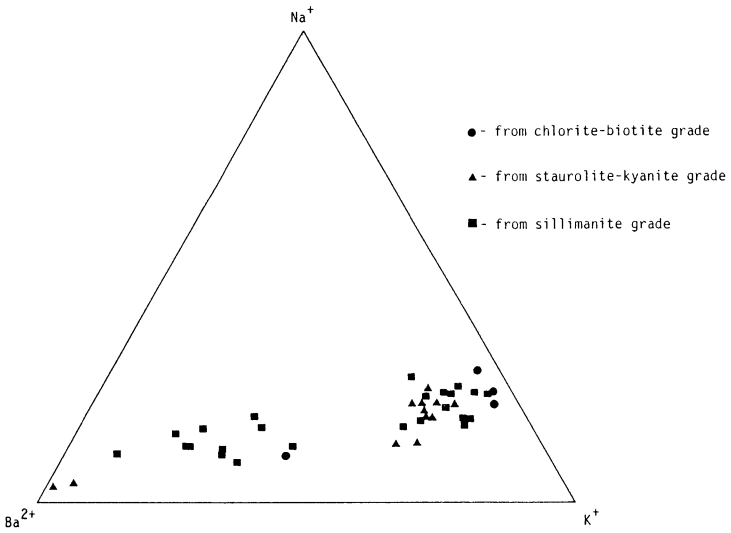

FIG. 3. Plots of the A-cations in hollandite and cryptomelane from various grades of metamorphism. Published data of Bhattacharya *et al.* (1984) are included.

A similar feature is observed in the supergene cryptomelane of this belt. Figure 2 shows the colour macromaps of Ba^{2+} and K^{+} in hollandite-cryptomelane series, formed along the cracks of braunite. Cryptomelane is a supergene mineral derived from braunite. As the total oxide content of this cryptomelane is only 90 – 91wt% (Table 5), this phase may contain nearly 10% H_2O. The distribution pattern of Ba^{2+} and K^{+} ions also reveals that these two elements exist separately and do not show continuous replacement.

Miura (1986) and Post *et al.* (1982) who studied on single crystals have reported anhydrous hollandite and cryptomelane respectively from this belt. They found monoclinic nature of these two minerals. In the present study, however, both monoclinic and tetragonal structures of these phases were observed, independent of the metamorphic grade. In order to know the relationship between crystal symmetry of hollandite-cryptomelane series and chemical composition (especially, species of A-cation and site occupancies), the cell constants of some single grains were measured. Samples were chosen from Tirodi area of the Sausar belt. The diffraction data were obtained by Rigaku AFC-5UD four-circle goniometer with Mo-Kα monochromatized

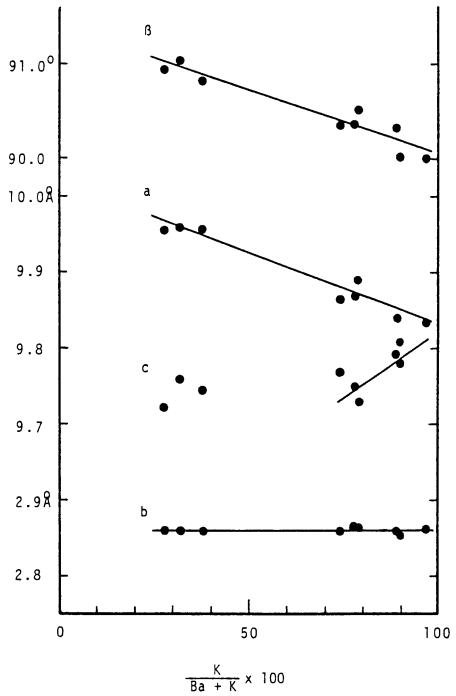

FIG. 4. Relation between cell dimensions and K/(K+Ba) of hollandite and cryptomelane from Tirodi mine.

by pyrolytic graphite. The unit cell constants were determined using 12-16 reflections. Least square calculations were performed by URAP program (Rigaku). Chemical composition of each grain were analyzed by EPMA. The results are shown in Fig. 4. There is a clear correlation between K/(Ba + K) ratio and β angle. With increasing K^+ content, β angle decreases from 91.1° (monoclinic) to 90.0° (tetragonal). The length of the a-axis also shows a clear correlation to K/(Ba + K) ratio. Though the length of the b-axis is almost constant. Within the range of K/(Ba + K) = 0.7 and 0.95 (cryptomelane), the c-axis increases with increasing of K^+ content. The c-axis of hollandite can not plot on the extrapolated line of that of cryptomelane solid solution. Thus it can be said that the crystal symmetry of hollandite-cryptomelane series in Tirodi area is controlled by the composition of the A-cation.

Discussion

In Precambrian Sausar group of India, the hollandite/cryptomelane + braunite ±bixbyite bearing assemblages studied here were stable in a wide range of metamorphism, from the lowest to the highest grade, attained by the rocks of this group. Bhattacharya *et al.* (1984) reported that Ba^{2+} ions stabilized the hollandite phase at a high grade of metamorphism such as sillimanite grade of the Tirodi area. Similarly K^+ cation as well as Ba^{2+} in the tunnel structure will stabilize the cryptomelane phase at similar grade of metamorphism (Burns and Burns, 1977). Hollandite or cryptomelane formed in the late diagenetic stage and remained as stable phases upto the highest grade of metamorphism in the belt. High K^+ ion content of cryptomelane which was formed irrespective of the presence of K-feldspar (Table 1) can not also be ascribed to high metasomatic concentration of alkali elements. Hollandite found in the pegmatite veins in this area does not show any appreciable compositional change from other occurrences (Table 4).

The crystal symmetry of these phases depended on the available K/(Ba + K) ratio. Post et al. (1982) pointed out that the crystal symmetry of α-MnO_2 series minerals depends on the relative ionic radii ratio of A-cation to the metallic ion which forms the framework. In hollandite-cryptomelane series, average radii of Ba^{2+} ion is nearly the same to that of K^+ ion. The difference in the electric charge of these cations is believed to give a great effect to crystal symmetry and there is only a limited extent of mutual replacement of the tunnel cations within a particular phase. The effect of metamorphic grade to the crystal symmetry of cryptomelane-hollandite series minerals may be minor.

The breakdown of hollandite to hausmannite +Ba-feldspar observed in the present region (Bhattacharya *et al.*, 1984) can not simply be explained by the P-T condition of metamorphism. It has already been established that the f_{O_2} conditions of the

TABLE 4. Chemical composition of hollandite from pegmatite veins.

Serial No.	1	2
Sample No.	TI7	TI7'
SiO_2	0.00	0.00
TiO_2	0.40	0.45
Al_2O_3	0.21	0.25
Cr_2O_3	0.00	0.00
Fe_2O_3	7.73	7.80
MnO_2	75.04	73.43
MgO	0.00	0.03
NiO	0.00	0.09
CaO	0.02	0.02
Na_2O	0.52	0.37
K_2O	0.99	0.54
BaO	11.58	14.16
Total	96.49	97.14
Si	0.000	0.000
Ti	0.041	0.045
Al	0.033	0.040
Cr	0.000	0.000
Fe^{3+}	0.782	0.797
Mn^{4+}	6.966	6.892
Mg	0.000	0.007
Ni	0.000	0.009
Ca	0.003	0.003
Na	0.134	0.098
K	0.170	0.093
Ba	0.609	0.754
Total	8.738	8.738

Note: Number of ions calculated on O = 16. Total Mn as MnO_2 and Fe as Fe_2O_3.

TABLE 5. Chemical composition of supergene cryptomelane.

Serial No.	1	2
Sample No.	TI1	TI4
SiO_2	0.14	0.00
TiO_2	0.48	0.00
Al_2O_3	0.22	0.01
Cr_2O_3	0.00	0.02
Fe_2O_3	18.47	9.02
MnO_2	66.54	76.68
MgO	0.04	0.00
NiO	0.00	0.00
CaO	0.39	0.44
Na_2O	0.27	0.27
K_2O	4.22	5.00
BaO	0.10	0.00
Total	90.87	91.44
Si	0.020	0.000
Ti	0.049	0.000
Al	0.035	0.002
Cr	0.000	0.002
Fe^{3+}	1.890	0.904
Mn^{4+}	6.253	7.058
Mg	0.008	0.001
Ni	0.000	0.000
Ca	0.056	0.063
Na	0.072	0.070
K	0.731	0.850
Ba	0.005	0.000
Total	9.119	8.950

Note: Number of ions calculated on O = 16. Total Mn as MnO_2 and Fe as Fe_2O_3.

manganese oxide assemblages varied widely (Dasgupta and Manickavasagam, 1981) and was buffered internally by the mineral assemblages (Dasgupta *et al.*, 1985). With rising temperature, in an isobaric situation, the f_{O_2}-T path must have intersected the bixbyite-hausmannite buffer curve and shifted into the hausmannite stability field. We believe that the breakdown of hollandite into hausmannite-bearing assemblage can easily happen simply by the change of f_{O_2} condition of the system during metamorphism.

Acknowledgements—We thank Mr. Terada and Mr. Kuwajima of Hokkaido University for the preparation of the EPMA sample.

References

BHATTACHARYA, P.K., DASGUPTA, S., FUKUOKA, M. and ROY, S. (1984) *Contr. Min. Pet.*, **87**, 65-71.

BURNS, R.G. and BURNS, V.M. (1977) *Mineralogy. In: Glosby G.P. (Editors), Marine Manganese Deposits*, Elsevier, Amsterdam, 185-248.

BURNS, R.G., BURNS, V.M. and STOCKMAN, H.W. (1983) *Am. Miner.*, **68**, 972-980.

BURNS, R.G., BURNS, V.M. and STOCKMAN, H.W. (1985) *Am. Miner.*, **70**, 205-208.

BYSTRÖM, A. and BYSTRÖM, A.M. (1950) *Acta Cryst.*, **3**, 146-154.

BYSTRÖM, A. and BYSTRÖM, A.M. (1951) *Acta Cryst.*, **4**, 469.

DASGUPTA, H. and MANICKAVASAGAM, R.M. (1981) *Jour. Petrol.*, **22**, 363-396.

DASGUPTA, S., BANERJEE, H. and MAZUMDAR, N. (1984) *N. Jb. Miner. Abh.*, **150**, 95-102.

DASGUPTA, S., BANERJEE, H. and FUKUOKA, M. (1985) *Contrb. Miner. Petrol.*, **90**, 258-261.

GIOVANOLI, R. (1980) *In: 2nd MnO_2 Symposium, Tokyo, 1980. Japanese Electrochemical Society*, pp. 45-50.

GIOVANOLI, R. and BALMER, B. (1981) *Chimia*, **5**, 53-55.

MIURA, H. (1986) *Miner. Jour.*, **13**, 119-129.

NAMBU, M. and TANIDA, K. (1980) *Jour. Miner. Soc. Japan*, **14**, 62-85.

POST, J.E., Von DREELE, R.B. and BUSECK, P.R. (1982) *Acta Cryst.*, **B38**, 1056-1065.

ROY, S. (1966) *Syngenetic Manganese Formations of India. Jadavpur University, Calcutta*, 219 pp.

ROY, S. (1981) *Manganese Deposits*. Academic Press, London, 458 pp.

TURNER, S. and BUSECK, P.R. (1979) *Science*, **203**, 456-458.

TURNER, S. and BUSECK, P.R. (1981) *Science*, **212**, 1024-1026.

Received January 30, 1987; revised March 31, 1987.